Journal of Peptide Science
J. Peptide Sci. **4**: 344–354 (1998)

Influence of the Secondary Structure on the Pore Forming Properties of Synthetic Alamethicin Analogs: NMR and Molecular Modelling Studies

LAURENT BRACHAIS[a], CATHERINE MAYER[b], DANIEL DAVOUST[b] and GÉRARD MOLLE[a,*]

[a] UMR 6522 CNRS, IFRMP 23, Faculté des Sciences de Rouen, Université de Rouen, 76821 Mont Saint Aignan Cedex, France
[b] Centre Régional Universitaire de Spectroscopie, UPRESA 6014 CNRS, IFRMP 23, Université de Rouen, 76821 Mont Saint Aignan Cedex, France

Received 28 July 1997
Accepted 30 October 1997

Abstract: Synthetic alamethicin analogs, in which all Aib residues had been replaced by Leu (L2) then proline 14 replaced by an alanine (L5), were studied in SDS micelles using circular dichroism and NMR spectroscopy. Nuclear Overhauser effects were used as constraints for molecular modelling. The structures determined for both peptides in SDS micelles were compared with those previously obtained in methanol in order to establish a secondary structure/ionophore activity relationship. Our results indicated that a shortening of peptide helices could be responsible for the observed decrease in ion channel lifetimes. However, the length of helices may not by itself explain the drastic destabilization of channels when Pro14 of alamethicin is replaced by Ala in L5. Indeed analysis of the helical wheel of L5 reveals heterogeneity in the amphipathicity depending on the medium. Thus, loss of amphipathicity seems to underly the observed destabilization of channels. © 1998 European Peptide Society and John Wiley & Sons, Ltd.

Keywords: ion channels; amphipathicity; α-helices; bilayers; SDS micelles

INTRODUCTION

Alamethicin, a 20-residue peptaibol from fungus *Trichoderma viride* [1], has been extensively studied, because it induces voltage-dependent channels in lipid bilayers [2–7]. Even if conductance properties agree with the well-known barrel-stave model, built from amphipathic helices [8], the mechanism for channel gating has not yet been established. Several mechanisms have been suggested [3,9–11]. According to a detailed X-ray crystallographic study, Fox and Richards [11] suggested a model of helical association, as well as an opening mechanism which takes advantage of the kink induced by Pro14 in the alamethicin structure. As a matter of fact, Pro14 and several other residues like Gln7 or Glu18 seem to play an important role in channel formation, since they can be found at analogous positions in the sequence of most peptaibols which exhibit ionophore properties. Synthetic analogs of alamethicin have been studied for years in our laboratory in order to establish clearly the role of these key residues [12]. We have shown that Aib residues of this peptaibol are not involved in the voltage-dependence, since their replacement by Leu leads to voltage-gated channels (analog L2) [13,14]. However, a decrease in channel lifetimes can be observed for L2 as compared to alamethicin. Several hypotheses can be proposed as an explanation for such behavior:

First, steric interactions induced by bulky lateral chains of Leu could explain this decrease. Nevertheless, the replacement in L2 of Leu3 by Ala, i.e. in the area where the helices may interact, does not increase the channel lifetimes. This suggests that the destabilization of the channels does not involve modifications of interactions between helices [15].

* Correspondence to: UMR 6522 CNRS, IFRMP 23, Faculté des Sciences de Rouen, 76821 Mont Saint Aignan Cedex, France.

CCC 1075–2617/98/050344-11$17.50

A difference in the length of the helices of alamethicin and L2 could also be responsible for the channel lifetime decrease. The conductance study of a lengthened analog supports this hypothesis since this analog has greater channel lifetimes than those of L2 [12]. Moreover, a previous conformational study of L2 in methanol solution was in favour of this hypothesis [16,17]. Molecular modelling using NMR constraints showed that L2 has a greater α-helical content than alamethicin which includes some 3_{10} helical parts in its structure.

In the same way, the involvement of Pro14 in the voltage-gating has also been investigated. This residue was substituted by Ala in the L2 sequence to produce a new analog (L5). Conductance studies performed with L5 indicate that the voltage-dependence is retained in the absence of Pro14 [18]. However, a drastic destabilization of the channels which might be induced by a shorter α helix, was observed with respect to L2. Previous conformational studies of L2 and L5 have been carried out in methanol solutions and allowed us to record high resolved NMR spectra.

In the present study, new experiments on L2 and L5 were undertaken in SDS micelles. Micelles, while clearly not membranes, provide a heterogeneous environment that is closer to that of a bilayer than bulk solvents such as methanol [19].

This paper presents a detailed comparison between the structures of alamethicin analogs (L2 and L5) in methanol and in SDS micelles. Molecular modelling of these analogs appears to be a promising way to study the modulation of ion channel lifetime and should allow a better understanding of the voltage-gated mechanism of alamethicin.

Alamethicin and Related Synthetic Analogs

Alamethicin: Ac-Aib-Pro-Aib-Ala-Aib-Ala-Gln-Aib-Val-Aib-Gly-Leu-Aib-Pro-Val-Aib-Aib-Glu-Gln-Pheol.
L2: Ac-Leu-Pro-Leu-Ala-Leu-Ala-Gln-Leu-Val-Leu-Gly-Leu-Leu-**Pro**-Val-Leu-Leu-Glu-Gln-Pheol.
L5: Ac-Leu-Pro-Leu-Ala-Leu-Ala-Gln-Leu-Val-Leu-Gly-Leu-Leu-**Ala**-Val-Leu-Leu-Glu-Gln-Pheol.

MATERIALS AND METHODS

Peptide Synthesis and Purification

Both synthetic alamethicin analogs were prepared by the solid-phase technique [20]. In order to obtain an amino-alcohol at the C-terminus, a protocol described previously [21] for amidated peptides, was modified [22].

After synthesis and acetylation of the N-terminus, the peptide was released from the resin by a saponification reaction instead of the usual HF treatment. The lyophilised raw products were purified by HPLC (LKB system) through repeated steps on an inverse phase column (C-8, 5 μm, 4.6 × 250 mm; from Société Française Chromato Colonne) under MeOH/H_2O or EtOH/H_2O gradients.

Fast atomic bombardment (FAB) positive ion mass spectrometry allowed an unambiguous characterization [23] of the purified peptides. Examination of the fragment masses from both C-terminus (B-type ions) and from N-terminus (Y-type ions), as well as the protonated molecular ion, confirms the sequence generated during the chemical synthesis.

Conformational Study

CD measurements in 8% SDS solutions were performed with a Mark V Jobin Yvon dichrograph, at 1 nm resolution and at room temperature; the peptide concentration was 1 mg/ml and the optical path 0.01 cm. Ten scans were recorded at the speed of one point every 2 s. Elucidation of the conformations was performed using the CD reference curves of Yang *et al.* [24,25]. These calculations were obtained from a custom made program using the conventional additivity rule between 190 and 240 nm at every nanometer. All conformations were first computed to within 5%. The resulting theoretical curves were subtracted from the experimental one and the least squares method was used to choose the best fit. Then a more precise computation was achieved to within 1% of the best estimation of the first approach.

Samples for NMR experiments were prepared by dissolving a mixture of 4 mg of peptide and 32 mg of perdeuterated SDS (from the Commissariat à l'Energie Atomique, France) in 0.4 ml H_2O/D_2O (90/10). NMR experiments were carried out at 303 K because the greatest dispersion and resolution of the NH signals were observed at this temperature.

^{1}H NMR spectra were recorded at 400.13 MHz on a Bruker ARX400 spectrometer fitted with an Aspect X32 computer. The spectra, referenced to water resonance at 4.75 ppm down field from TMS, were obtained by solvent presaturation. One dimensional ^{1}H spectra were performed with 16 K data points using quadrature phase detection, a 90° pulse, a relaxation delay of 2 s between scans and a spectral width of 4000 Hz.

Table 1 Summary of the Molecular Modelling Procedure used to Compute the Structures of L2 and L5 in Methanol and SDS Micelles

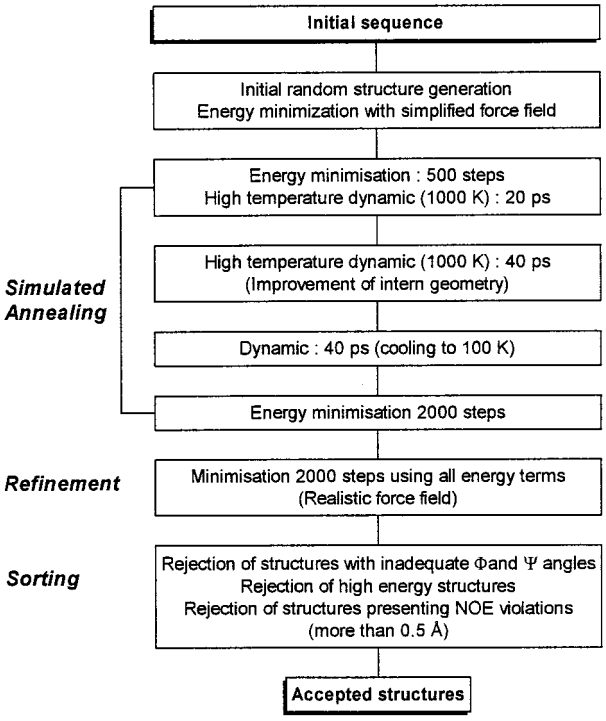

For each peptide, 100 structures were computed in each medium. After the final sort, only the 20 lowest energy structures were taken into consideration.

Standard methods were used to perform the two-dimensional experiments, pulse programs being taken from the Bruker software library. For TOCSY and NOESY, a total of 512 increments were acquired with sweep width in F2 of 4000 Hz and 64 scans per t_1 increment (size 2 K); zero filling to 1 K was applied in F1. A $\pi/2$ shifted sine-bell function was applied on FIDs prior to Fourier transform. For TOCSY, a MLEV 17 sequence [26] was used with a mixing time of 60 ms. NOESY experiments were achieved with mixing times of 200, 300, 400 and 500 ms.

Molecular Modelling

NMR constraints for the molecular modelling studies were quantified from the 300 ms mixing time NOESY experiment which allowed to observe the maximum NOE informations with a low spin diffusion. A conformational model was designed by simultaneously optimizing the experimental parameters: NOEs related to internuclear distances and the intramolecular energy. The latter was calculated by using X-PLOR program from Brünger [27]. Calculations were performed on 4D380 and IRIS 4D210 Silicon Graphics workstations. The X-PLOR program was used with standard parameters for the internal geometry including bond stretching, bond angle bending, harmonic dihedral bending, Van der Waals, and electrostatic interactions in the potential energy function [28]. A constraint potential term was added to allow the molecule to satisfy the equation of NOE distance constraints: $\mathrm{NOE} = K(d - d_0)^2$, where K is a weighting factor (50 kcal/mol), d is the actual distance between atoms i and j, and d_0 the given constraint for this pair. The protocol automatically generates a template coordinate set. The coordinates are then regularized using simulated annealing. Computation strategy used to solve three-dimensional structures on the basis of NMR data is summarized in Table 1 and are carried out without using a solvent box (implicite solvent), since NOE data already take into account the presence of solvent.

From ten different template coordinates, 100 structures were generated. Then the protocol produced a subfamily of accepted coordinates for which the NOE distances were different from the distance boundaries by no more than 0.5 Å, the dihedral angle restraint violations were lower than 0.01 Å, and the RMSD angles were lower than 1°. The configurations corresponding to inadequate Φ and Ψ couples (Ramachandran map) were excluded. The final structures were refined during minimisation step whose energy function included all terms. Representations of the molecules were drawn using SYBYL (TRIPOS Associates) and MOLSCRIPT [29].

RESULTS AND DISCUSSION

Circular Dichroism

CD curves obtained with L2 and L5, reported on Figure 1, show a strong positive (192 nm) and two negative (208 and 222 nm) Cotton effects which are characteristic of a largely helical conformation. Moreover, the amounts of different conformations can be obtained from CD reference curves of proteins with well-known X-ray structures. Several set of curves are available and those described by Yang *et al.* [25] from 190 to 240 nm (with 1 nm step) were chosen because they take into account four different conformations (helix, β-sheet, β-turn and random coil). These reference curves, previously used in the computation of L2 and L5 structures in

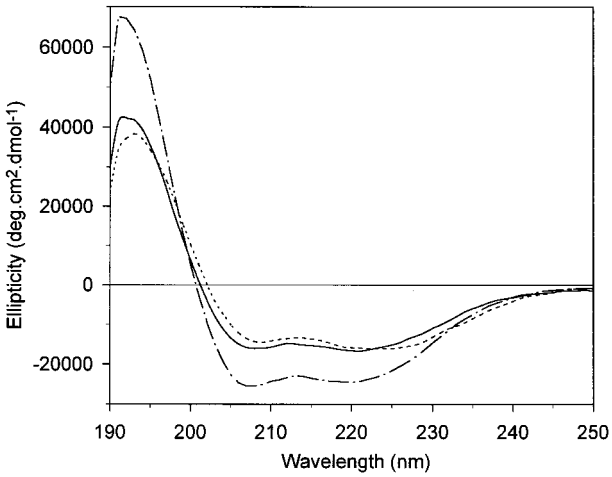

Figure 1 CD spectra of alamethicin (dotted line), L2 (solid line) and L5 (dashed dotted line) at room temperature in SDS micelles, obtained at 1 mg/ml concentration in 0.01 cm quartz cells.

methanol [16,17], provided fairly good deviations (RMSD). Results of computations obtained from the curves of L2, L5 and alamethicin in SDS micelles are reported in Table 2 as well as those previously obtained in methanol for comparison. In both media, peptides exhibit a dominant helical structure. However, SDS micelles seem to increase the helical content with respect to methanol.

L5 is the most helical peptide in both media (72% in SDS and 61% in methanol). Such a result was expected since the substitution of Pro14 by Ala allows an additional H-bond which stabilizes the helix in the C-terminal part. Alamethicin, the less helical peptide in methanol, is more helical than L2 in SDS. However, RMSD values reported in Table 2 are not negligible (8–15%) and comparison of peptides structures from this table has to be considered carefully. The helical contents increase in SDS micelles as regard to methanol while the random coil content decreases for all peptides. No significant change can be detected for the β-sheet and β-turn conformations between both media. Thus, our data show that SDS micelles stabilize the helices of the three peptides, but conclusions on detailed conformations are difficult to draw from the CD studies alone.

NMR Spectroscopy

NMR studies were performed in SDS micelles at 303 K since the highest dispersion of amide proton signals was obtained for both peptides around this temperature, making the resonance assignments easier. The complete interpretation of the one-dimensional proton spectra could be achieved using two-dimensional correlated NMR spectroscopies. Initially, ^{1}H spin systems were determined by total correlation spectroscopy (TOCSY). Most of the spin systems were determined using correlations between amide protons and other protons as shown for L5 on Figure 2. Assignment problems due to overlapping of amide protons and in the determination of prolines spin systems could be solved by the complete analysis of TOCSY spectra. For further sequential assignment of the 20 spin systems found for each peptide, a NOESY experiment was employed. Taking advantage of the largely helical structure of the peptides, this interpretation could be conducted by observing dNN(i, $i+$l) NOEs. The starting residue for both peptides was the unambiguously assigned Pheol20 (existing only once in each sequence). It was possible to rebuild the L5 sequence, residue by residue, down to Leu3 (Figure 3). For L2, the presence of prolines prevented the sequential assignment after Vall5 and Leu3. Nevertheless, other correlations from the NOESY spectrum could be used to assign prolines spin systems. All sequential assignments could be then verified by

Table 2 Calculated Secondary Structures of L2, L5 and Alamethicin from CD Measurements at Room Temperature, using Reference curves of Yang *et al.* [25] every nanometer between 190 and 240 nm

Medium	Peptide	H (%)	B (%)	T (%)	R (%)	RMSD (%)
SDS	L2	63	15	0	22	11.6
	L5	72	0	0	28	14.2
	Alamethicin	70	8	4	18	8.2
MeOH	L2	55	9	0	36	13.0
	L5	61	0	0	39	12.4
	Alamethicin	49	21	5	25	11.7

H, B, T and R represent respectively helix, beta sheet, beta turn and random coil conformations. RMSD is the root mean square deviation

the dαN(i, $i+$l) NOE's. The proton chemical shifts of L2 and L5 are reported in Table 3 and assignments for the amide proton region are shown on Figure 4.

In the same way, we attempted to determine the configurations of prolines in both peptides. Only the *trans* configuration could be observed as indicated by the strong d$\alpha\delta\delta'$(i, $i+$l) NOEs between Leu1 and Pro2 (and also between Leul3 and Pro14 for L2).

For the following molecular dynamics computations, the assignment of NOESY spectra allowed the extraction of 140 and 153 distance constraints, for L2 and L5, respectively.

The most characteristic NOE data for both peptides, reported on Tables 4 and 5, confirm the largely helical structure of the analogs as shown by the dNN(i, $i+1$) and dαN(i, $i+3$) interactions observed all along the sequences. Moreover, the presence of dαN(i, $i+4$) and d$\alpha\beta$(i, $i+3$) together with few dαN(i, $i+2$) connectivities favours an α-helix rather than a 3_{10} helix [30]. The conformation of L2 around Pro14 is better defined in SDS micelles than in methanol. This result confirms the higher helicity found in the circular dichroism study.

However, a larger number of NOEs could be expected in SDS, according to the viscosity of this medium as compared to methanol. Because of the slower rotational correlation time for the peptide in micelles, cross-relaxation should be more efficient, in principle, leading to a better defined structure. Comparison of the conformations obtained in SDS micelles to those previously obtained in methanol is nevertheless difficult. Indeed, these preliminary data are not sufficient enough to suggest that a voltage-gating mechanism and molecular modelling studies become necessary.

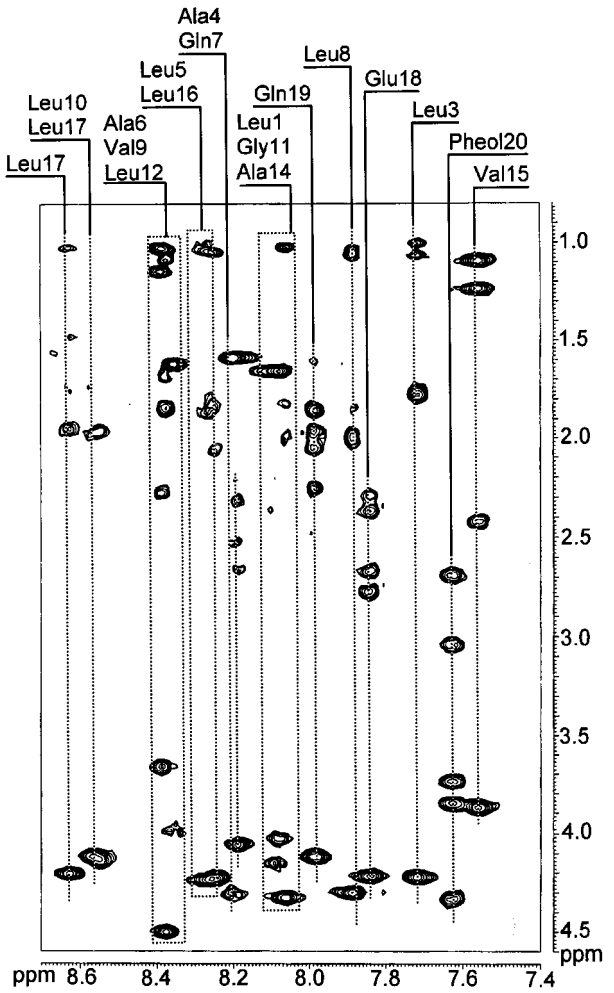

Figure 2 Part of a TOCSY spectrum of L5 (400.13 MHz, 303 K) in D_{25} SDS micelles, with a mixing time of 60 ms, showing correlations between amide protons ($\omega_2 = 8.7$–7.4 ppm) and other protons ($\omega_1 = 4.6$–0.8 ppm). This only area allowed the determination of most of the spin systems. Spin systems for which recoveries of NH signals were observed are boxed and were solved with other areas of the TOCSY experiments.

Molecular Modelling

From 100 computed structures for each peptide, 77 and 67 were accepted for L2 and L5, respectively and converged clearly to an α-helical conformation. The RMSD values ranged from 0.1 to 0.5 Å for L2 and from 0.2 to 0.9 Å for L5, indicating a better convergence of the structures of L2. The average energies of the accepted structures were -113 and -124 kcal/mol for L2 and L5, respectively. Superimposition of the ten lowest energy structures (not shown) gave for each peptide satisfactory results. Then, an average structure was computed for each analog in SDS as well as in methanol for comparison. Representations of these structures are drawn on Figures 5 and 6 in two different orientations.

In both media, the L2 helices show regular structures along their axis which are lightly bent near the Pro 14, although a higher flexibility was observed in methanol [17]. Actually, bending angle values of helices are low (less than 30°) and energy levels computed from the most bent helices and from straight helices are very similar. From this observation, it seems that applying a voltage would not be necessary for straightening the helices in planar lipid bilayers ruling out the voltage-gated mechanism suggested by Fox and Richards [11].

Table 3 Specific H Assignments (ppm) for Residues of L2 and L5 in SDS Micelles at 303 K

	L2			L5		
	NH	H_α	Other groups	NH	H_α	Other groups
Ac			Me = 2.01			Me = 2.01
Leu 1	8.41	4.49	$\beta = 1.88$; $\gamma = 1.71$; $\delta_1 = 1.06$; $\delta_2 = 1.11$	8.06	4.33	$\beta = 2.01$; $\gamma = 1.83$; $\delta_1 = 1.03$; $\delta_2 = 1.03$
Pro		4.38	$\beta_1 = 2.35$; $\beta_2 = 2.03$; $\gamma_1 = 2.13$; $\gamma_2 = 2.03$; $\delta_1 = 4.01$; $\delta_2 = 3.85$			$\beta_1 = 2.36$; $\beta_2 = 2.07$; $\gamma_1 = 2.30$; $\gamma_2 = 2.13$; $\delta_1 = 4.02$; $\delta_2 = 3.80$
Leu 3	7.66	4.23	$\beta = 1.80$; $\gamma = 1.80$; $\delta_1 = 1.02$; $\delta_2 = 1.07$	7.72	4.23	$\beta = 1.78$; $\gamma = 1.77$; $\delta_1 = 1.07$; $\delta_2 = 1.01$
Ala 4	8.15	4.31	$\beta = 1.61$	8.20	4.31	$\beta = 1.59$
Leu 5	8.35	4.24	$\beta = 1.88$; $\gamma = 1.78$; $\delta_1 = 1.00$; $\delta_2 = 1.05$	8.27	4.24	$\beta = 1.89$; $\gamma = 1.79$; $\delta_1 = 1.06$; $\delta_2 = 1.01$
Ala 6	8.33	4.01	$\beta = 1.64$	8.35	4.00	$\beta = 1.62$
Gln 7	8.20	4.06	$\beta_1 = 2.33$; $\beta_2 = 2.22$; $\gamma_1 = 2.69$; $\gamma_2 = 2.56$; $NH_2 = 7.35$ & 6.84	8.19	4.06	$\beta = 2.31$; $\beta_2 = 2.22$; $\gamma_1 = 2.67$; $\gamma_2 = 2.53$; $NH_2 = 7.35$ & 6.83
Leu 8	7.87	4.29	$\beta = 2.01$; $\gamma = 1.86$; $\delta_1 = 1.03$; $\delta_2 = 1.08$	7.89	4.30	$\beta = 2.02$; $\gamma = 1.98$; $\delta_1 = 1.07$; $\delta_2 = 1.04$
Val 9	8.26	3.68	$\beta = 2.30$; $\gamma_1 = 1.15$; $\gamma_2 = 1.03$	8.39	3.67	$\beta = 2.28$; $\gamma_1 = 1.15$; $\gamma_2 = 1.04$
Leu 10	8.47	4.18	$\beta = 1.93$; $\gamma = 1.72$; $\delta_1 = 1.03$; $\delta_2 = 1.03$	8.55	4.14	$\beta = 1.97$; $\gamma = 1.66$; $\delta_1 = 1.02$; $\delta_2 = 1.02$
Gly 11	8.01	4.25		8.08	4.03	
Leu 12	7.86	4.59	$\beta = 1.80$; $\gamma = 1.80$; $\delta_1 = 1.02$; $\delta_2 = 1.07$	8.38	4.50	$\beta = 1.85$; $\gamma = 1.70$; $\delta_1 = 1.09$; $\delta_2 = 1.05$
Leu 13	7.88	4.30	$\beta = 2.01$; $\gamma = 1.86$; $\delta_1 = 1.03$; $\delta_2 = 1.09$	8.57	4.12	$\beta = 1.98$; $\gamma = 1.74$; $\delta_1 = 0.97$; $\delta_2 = 0.97$
Pro14/Ala 14		4.38	$\beta_1 = 2.50$; $\beta_2 = 1.96$; $\gamma_1 = 2.23$; $\gamma_2 = 2.13$; $\delta_1 = 1.96$; $\gamma_1 = 2.23$	8.09	4.16	$\beta = 1.66$
Val 15	7.24	3.94	$\beta = 2.43$; $\gamma_1 = 1.11$; $\gamma_2 = 1.20$	7.55	3.88	$\beta = 2.42$; $\gamma_1 = 1.24$; $\gamma_2 = 1.09$
Leu 16	8.04	4.25	$\beta = 2.02$; $\gamma = 1.83$; $\delta_1 = 1.07$; $\delta_2 = 1.07$	8.24	4.23	$\beta = 2.09$; $\gamma = 1.83$; $\delta_1 = 1.06$; $\delta_2 = 1.06$
Leu 17	8.45	4.19	$\beta = 1.91$; $\gamma = 1.72$; $\delta_1 = 1.03$; $\delta_2 = 1.03$	8.63	4.20	$\beta = 1.96$; $\gamma = 1.76$; $\delta_1 = 1.04$; $\delta_2 = 1.04$
Glu 18	7.69	4.21	$\beta_1 = 2.31$; $\beta_2 = 2.27$; $\gamma_1 = 2.60$; $\gamma_2 = 2.54$	7.84	4.22	$\beta_1 = 2.37$; $\beta_2 = 2.29\gamma_1 = 2.78$; $\gamma_2 = 2.67$
Gln 19	7.86	4.09	$\beta_1 = 1.95$; $\beta_2 = 1.85$; $\gamma_1 = 2.22$; $\gamma_2 = 2.02$; $NH_2 = 7.10$ & 6.70	7.99	4.12	$\beta_1 = 1.97$; $\beta_2 = 1.86$; $\gamma_1 = 2.26$; $\gamma_2 = 2.06$; $NH_2 = 7.09$ & 6.72
Pheol 20	7.55	4.35	$\beta_1 = 3.04$; $\beta_2 = 2.69$; $CH_2OH = 3.85 = 3.85$ & 3.75 *ortho* = 7.42; *meta* = 7.34; *para* = 7.27	7.63	4.34	$\beta_1 = 3.04$; $\beta_2 = 2.69$; $CH_2OH = 3.85$ & 3.74 *ortho* = 7.42; *meta* = 7.33; *para* = 7.28

These assignments were obtained thanks to 2D TOCSY an NOESY experiments recorded on a 400 MHz spectrometer.

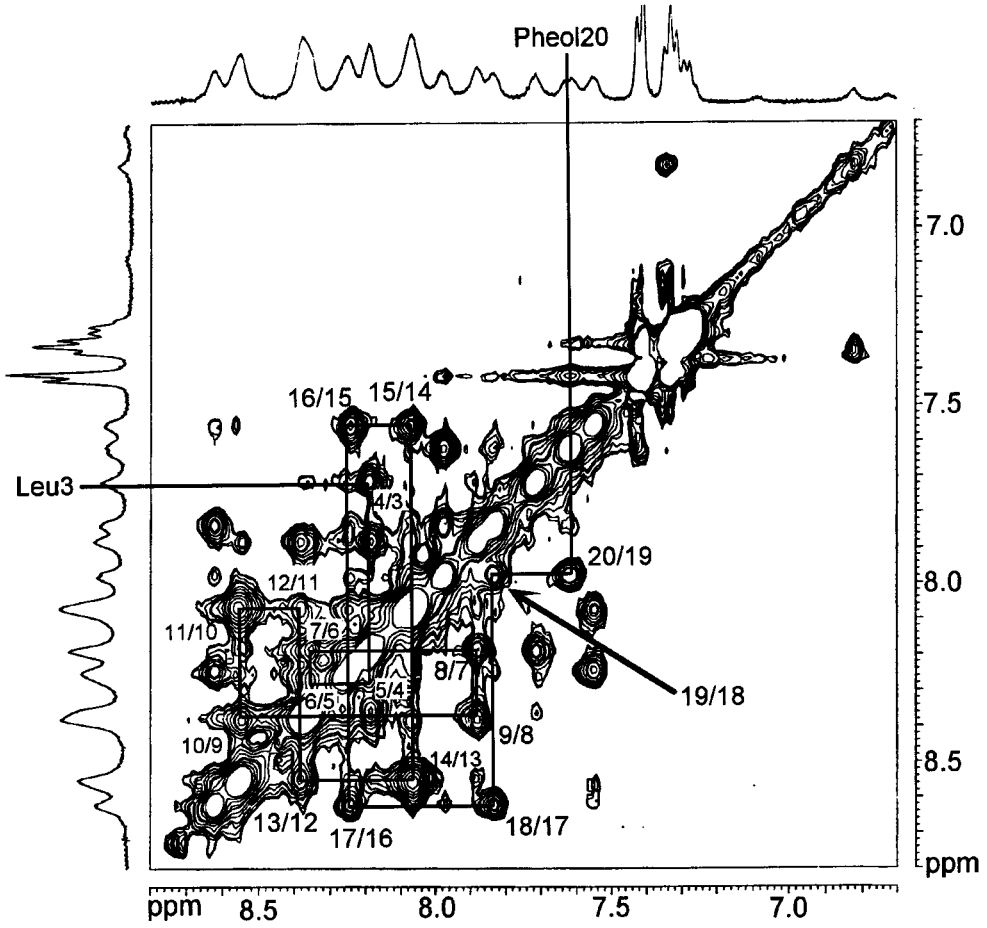

Figure 3 Part of a NOESY spectrum of L5 (400.13 MHz, 303 K) in D_{25} SDS micelles, with a mixing time of 300 ms. The shown region indicates the sequential connectivities between the backbone NH (8.8–6.7 ppm in both dimensions), labelled with the numbers of both involved residues. This sequential assignment could be obtained using the high helicity of the peptide.

L5 in methanol presents a less regular helix than L2 and some distortions are observed particularly in the C-terminal part. However, these distortions do not appear in SDS micelles. Thus, some heterogeneity of L5 conformation is observed according to the medium, even if a largely helical structure is conserved.

In our previous study [16], we showed that L2 had a greater α-helical content than alamethicin, resulting in a shorter length of L2. It is worthwhile comparing the lengths of alamethicin, L2 and L5 in methanol and SDS micelles. The length values reported in Table 6 were measured directly on the average structures, without taking into account both terminal acetyl and phenylalaninol, which are highly flexible areas. For alamethicin, the average structure obtained by X-ray determination was used (file from the Brookhaven Protein Data Bank). It has been previously shown that the average structure obtained by X-ray study for this peptaibol is very similar to the average structure computed from NMR data [31]. As expected, L2 is shorter than alamethicin since differences of 2.6 and 2.1 Å were found in methanol and SDS micelles, respectively. The decrease in length appears mainly in the C-terminal half. These measurements confirm our previous hypothesis mainly involving the lengths in the channel lifetimes. The lengths reported for L5 are also shorter than those reported for alamethicin in both media. However, comparison of the values of L5 and L2 shows a higher difference in methanol than in SDS micelles, where the lengths of both peptides are comparable. This confirms the heterogeneity of the structure of L5 depending on the

Table 4 Survey of L2 NOEs Connectivities Involving NH, Hα and Hβ Protons

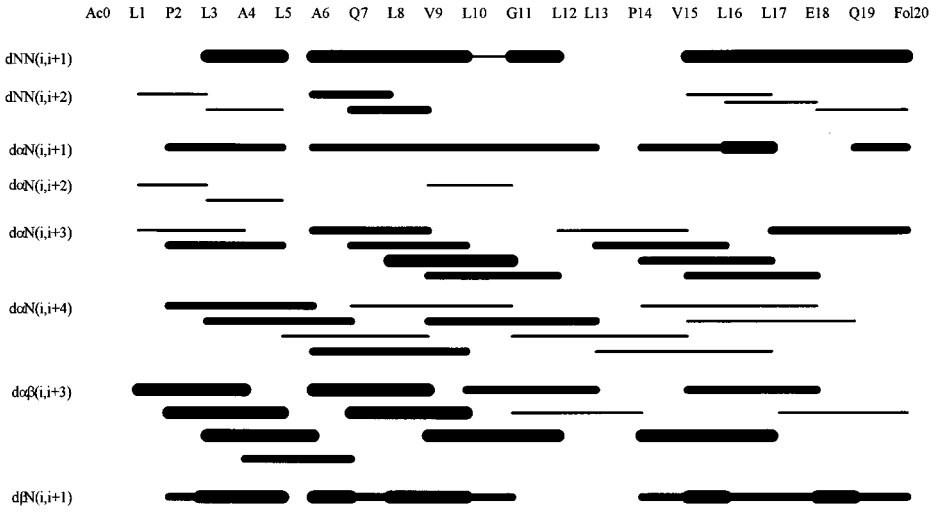

The observed NOEs are classified as strong, medium and weak (based on counting the contour plot levels) and shown by thick, medium and thin lines, respectively. These data were obtained at 400 MHz and 303 K with a mixing time of 300 ms.

medium. This could underlie the increased ion channel destabilization induced by this peptide. Differences in the structure could also influence the helices amphipathicities which are a critical parameter in the barrel-stave model. It was therefore interesting to study the position of the hydrophilic residues (Gln7 and Glu18) in schematic helical wheels with regard to this model. Average structures have been drawn perpendicularly to the helical axis with lateral chains of hydrophilic Gln7 and Glu18 residues (Figures 5 and 6). For L2 (Figure 5), coincidence between both lateral chains al-

Table 5 Survey of L5 NOEs Connectivities Involving NH, Hα and Hβ Protons

MHz and 303 K with a mixing time of 300 ms.

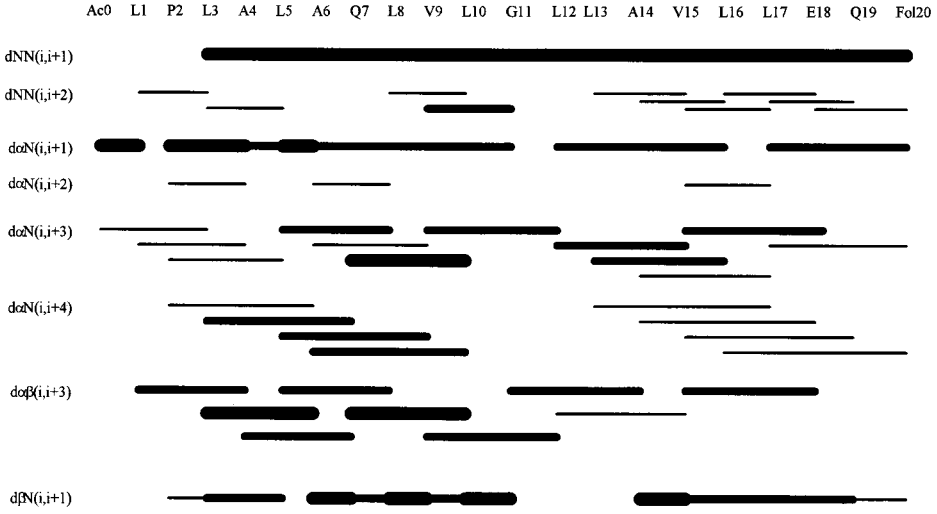

The observed NOEs are classified as strong, medium and weak (based on counting the contour plot levels) and shown by thick, medium and thin lines, respectively. These data were obtained at 400 MHz and 303 K with a mixing time of 300ms.

Table 6 Measured Lengths (in Å) for the Average Structures of Alamethicin, L2 and L5

Peptide	Médium	Cα1 to Cα10(N terminal half)	Cα10 to Cα19(C terminal half)	Cα1 to Cα19 all sequence
Alamethicin	X-ray	14.7	16.0	29.0
L2	Methanol	14.6	14.9	26.4
	SDS	13.5	14.6	26.9
L5	Methanol	13.9	12.1	25.0
	SDS	13.2	14.8	26.6

Measurements are made between α-carbons on both halves of peptides and on all the sequences, excluding terminal residues. Alamethicin measurements were done on the three molecules obtained in the crystallographic study [11] (Brookhaven Protein Data Bank); average values were then calculated. Both terminal acetyl and pheol were not included in these measurements, due to the high flexibility of both ends.

lows a good preservation of the amphipathicity in both media. In contrast, the high C-terminal distortion in the helix of L5 in methanol (Figure 6) induces the hydrophilic lateral chains projections in different directions, resulting in a loss of amphipathicity. This perturbation of the hydrophilic/hydrophobic sectors is not observed in SDS micelles.

A very strong destabilization of L5 channels would be the result of both peptide shortening and loss of amphipathicity. No conclusion can be drawn from the L5 structure obtained in SDS micelles since both length and amphipathicity are conserved, as compared to L2. Thus, in SDS, no conformational parameter is able to explain the channel destabilization observed from L2 to L5. In a previous detailed study, Vogel showed by Raman and circular dichroism that alamethicin has very similar structures in methanol and lipids [32]. Thus, this characteristic should also be expected with alamethicin analogues. Actually, the present study was carried out in SDS medium because this usually allows better defined structures than in organic solvents. From our data, it seems that SDS micelles are not ideal for mimicking lipid bilayers, even if they provide heterogeneous environment, close to that of lipids.

Several mechanisms have been proposed for the gating of alamethicin channels. If the consensus barrel-stave model is currently accepted, some questions concerning the voltage dependence are still not solved. Thus, some models like the voltage-dependent dipole [33,34], the voltage-dependent phase partitioning [35] or the voltage-dependent insertion [36] have been proposed. Nevertheless, additional control experiments do not agree with these different models [9]. Moreover, our results (same energy levels for the bent and straight helices) are in disagreement with the Fox and Richards model, where an applied voltage is necessary for the straightening of the bent helice [11]. Recently, Barranger-Mathys and Cafiso [37] proposed a model

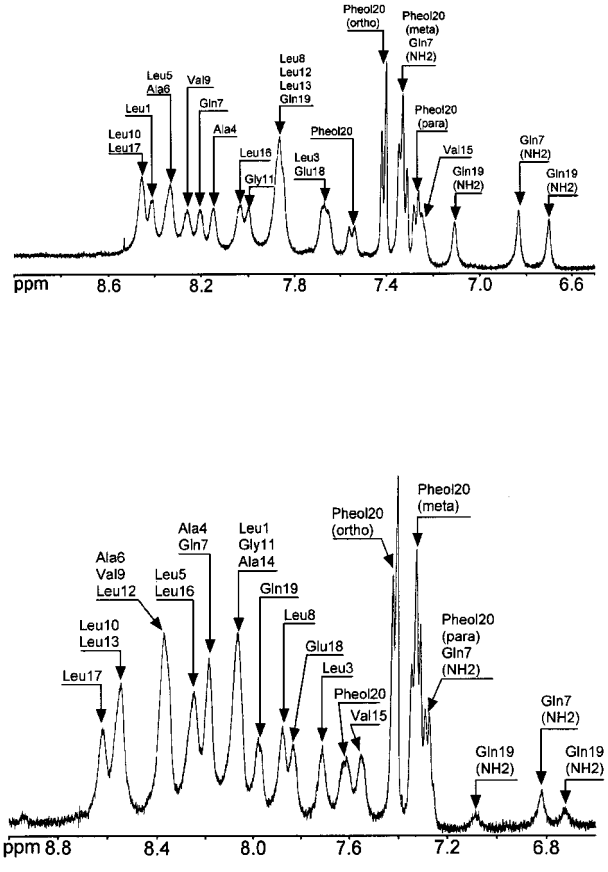

Figure 4 Low field regions of the 400 MHz ^{1}H NMR spectra of L2 (top) and L5 (bottom) in D_{25} SDS micelles at 303 K. The signals are labelled with the names and the positions of their respective residues. The apparent low resolution of the signals is due to the high viscosity and heterogeneity of SDS micelles.

where alamethicin would not completely cross the membrane at rest and application of voltage would result in the formation of an aggregate followed by its embedding in the lipid bilayer. However, it was not specified if the voltage gating was due to the association of monomers or to the complete insertion of the pre-aggregate. More recently, these authors confirmed by NMR and EPR studies [38,39] that alamethicin and L1 (an analog of L2 where Pheol is replaced by Phe-NH2) would be, under certain conditions of concentration and at rest, perpendicular to the plan of the bilayer with a greater embedding in the bilayer for L1 than for alamethicin. Nevertheless, our previous study with L1 [40] showed no significant voltage-gating difference in comparison with alamethicin. By inference from both studies, the determining step would not be the embedding of the aggregate, but the associative formation of different molecules of peptides. This hypothesis is supported by the study of Nishino *et al*. [41,42] who synthesized cyclic template-assembled alamethicins and showed that the ion channel formation was weakly voltage-dependent.

CONCLUSIONS

In conclusion, we showed that the replacement of Pro14 by Ala in L2 leads to the destabilization of the conducting aggregates which could be explained by the shortening of the alpha helix, but also by its loss of amphipathicity. Moreover, our results combined to recent studies indicate that the voltage-gating would mainly result from the formation of the aggregate in the bilayer.

Acknowledgements

We thank Jean-Yves Dugast for peptide synthesis. L. Brachais thanks the Conseil Regional de Haute Normandie for a doctoral fellowship. We are grateful for the financial support from GDR 1153 of CNRS.

REFERENCES

1. C.E. Meyer and F. Ruesser (1967). A polypeptide antibacterial agent isolated from *Trichoderma viride*. *Experientia 23*, 85–86.
2. G. Boheim (1974). Statistical analysis of alamethicin channels in black lipid membranes. *J. Membr. Biol. 19*, 277–303.
3. M.S.P. Sansom (1993). Alamethicin and related peptaibols. *Eur. Biophys. J. 22*, 105–124.
4. J.E. Hall and I. Vodyanoy (1984). Alamethicin: a rich model for channel behavior. *Biophys. J. 45*, 233–247.
5. W. Hanke and G. Boheim (1980). The lowest conductance state of the alamethicin pore. *Biochim. Biophys. Acta 596*, 456–462.
6. L.G.M. Gordon and D.A. Haydon (1975). Potential-dependent conductances in lipid membranes containing alamethicin. *Phil. Trans. R. Soc. London B 270*, 433–447.
7. I. Vodyanoy, J.E. Hall and T.M. Balasubramanian (1983). Alamethicin-induced current–voltage curve asymmetry in lipid bilayers. *Biophys. J. 42*, 71–82.
8. G. Boheim, W. Hanke and G. Jung (1983). Alamethicin pore formation: voltage dependent flip-flop of a-helix dipoles. *Biophys. Struct. Mech. 9*, 181–191.
9. D.S. Cafiso (1994). Alamethicin: a peptide model for voltage gating and protein-membrane interactions. *Ann. Rev. Biomolec. Struct. 23*, 141–165.
10. M.S.P. Sansom (1993). Alamethicin and related peptaibols-model ion channels. *Q. Rev. Biophys. 26*, 365–421.
11. R.O. Fox and F.M. Richards (1982). A voltage-gated ion channels model inferred from the crystal structure of alamethicin. *Nature 300*, 325–330.
12. G. Molle, H. Duclohier, J.-Y. Dugast and G. Spach (1989). Design and conformation of non-Aib synthetic peptides enjoying alamethicin-like ionophore activity. *Biopolymers 28*, 273–283.
13. G. Spach, H. Duclohier and G. Molle. Modulation of ionophore properties by chemical modifications of alamethicin synthetic analogues, in: *Transport through Membranes: Carriers. Channels and pumps – The 21st Jerusalem Symposium in Quantum Chemistry and Biochemistry*, A. Pullman, B. Pullman and P. Jortner, Eds., p. 67–76, D. Reidel Publishing, Amsterdam, 1988.
14. G. Molle, H. Duclohier, S. Julien and G. Spach (1991). Synthetic analogues of alamethicin: effect of C-terminal residue substitutions and chain lenght on the ion channel lifetimes. *Biochim. Biophys. Acta 1064*, 365–369.
15. G. Molle, H. Duclohier, J.-Y. Dugast and G. Spach. Influence of helix-helix contact on the stability of ion channels induced by a synthetic analogue of alamethicin, in: *Peptides 1992*. C. H. Schneider and A. N. Eberle (Eds.), p. 917–918, ESCOM Science Publishers B.V., 1993.
16. L. Brachais, D. Davoust and G. Molle (1995). Conformational study of a synthetic analogue of alamethicin: influence of the conformation on ion-channel lifetimes. *Int. J. Peptide Protein Res. 45*, 164–172.
17. L. Brachais L, H. Duclohier, C. Mayer, D. Davoust and G. Molle (1995) Influence of proline-14 substitution on the secondary structure in a synthetic analogue of alamethicin. *Biopolymers 36*, 547–558.

18. H. Duclohier, G. Molle, J.-Y. Dugast and G. Spach (1992) Prolines are not essential residues in the barrel-stave model for ion channel induced by alamethicin analogues. *Biophys. J. 63*, 868–873.
19. J.C. Franklin, J.F. Ellena, S. Jayasinghe, L.P. Kelsh and D.S. Cafiso (1994). Structure of micelle-associated alamethicin from ^{1}H NMR. Evidence for conformational heterogeneity in a voltage-gated peptide. *Biochemistry 33*, 4036–4045.
20. R.B. Merrifield (1963). Solid phase peptide synthesis: I The synthesis of a tetrapeptide. *J. Am. Chem. Soc. 89*, 2149–2154.
21. G. Molle G, J.-Y. Dugast, H. Duclohier, P. Daumas, F. Heitz and G. Spach (1988). Ionophore properties of a synthetic alpha-helical transmembrane fragment of the mitochondrial HF ATP synthetase of Saccharomyces cerevisiae. *Biophys. J. 53*, 193–203.
22. G. Molle and J.-Y. Dugast (1990). Synthèse sur support solide de peptide comportant un residu aminoalcool C-terminal. *Tetrahedron Lett. 31*, 6355–6356.
23. T.D. Lee in: *Methods of protein microcharacterisation*. J.E. Shively, Ed., p. 403–441, The Human Press Clifton, N.J., 1986.
24. C.T. Chang, C.-S.C. Wu and J.T. Yang (1978). Circular dichroic analysis of protein conformation: inclusion of the β-turns. *Anal. Biochem. 91*, 13–31.
25. J.T. Yang, C.-S.C. Wu. and H.M. Martinez (1986). Calculation of protein conformation from circular dichroism. *Methods Enzymol. 130*, 208–269.
26. D.F. Davis and A. Bax (1985) Simplification of ^{1}H NMR spectra by selective excitation of experimental subspectra. *J. Am. Chem. Soc. 107*, 7197–7198.
27. A.T. Brünger. *The X-PLOR software manual version 3.1*. Yale University, New Haven, CT, 1992.
28. B.R. Brooks, R.E. Bruccoleri, B.D. Olafson, D.J. States, S. Swaminathan and M. Karplus (1983). CHARMM: a program for macromolecular energy, minimization and dynamics calculations. *J. Comp. Chem. 4*, 187–217.
29. P. Kraulis (1991). MOLSCRIPT: a program to produce both detailed and schematic plots of protein structures. *J. Appl. Crystallogr. 24*, 946–950.
30. K. Wüthrich (1986). *NMR of Proteins and Nucleic Acids*, John Wiley and Sons, New York, 162–175.
31. A.A. Yee, R. Babiuk and J.D.J. O'Neil (1995). The conformation of an alamethicin in methanol by multinuclear NMR spectroscopy and distance geometry/simulated annealing. *Biopolymers 36*, 781–792.
32. H. Vogel (1987). Comparison of the conformation and orientation of alamethicin and melittin in lipid membranes. *Biochemistry 26*, 4562–4572.
33. G. Boheim, W. Hanke and G. Jung (1983). Alamethicin pore formation: voltage-dependent flip-flop of a-helix dipole. *Biophys. Struct. Mech 2*, 181–191.
34. M.K. Mathew and P. Balaram (1983). A helix dipole model for alamethicin and related transmembrane channels. *FEBS Lett. 157*, 1–5.
35. V. Rizzo, S. Stankowski and G. Schwarz (1987). Alamethicin incorporation in lipid bilayers: a thermodynamic analysis. *Biochemistry 26*, 2751–2759.
36. G. Baumann and P. Mueller (1974). A molecular model of membrane excitability. *J. Supramol. Struct. 2*, 538–557.
37. M. Barranger-Mathys and D.S. Cafiso (1996). Membrane structure of voltage-gated channel forming peptides by site-directed spin labeling. *Biochemistry 35*, 498–505.
38. J. Jacob and D.S. Cafiso (1997). Mechanism of voltage-gating in alamethicin: NMR studies of structural variance. *Biophys. J. 72*, A398.
39. S. Jayasinghe, M. Barranger-Mathys, J. Ellena, C. Franklin and D.S. Cafiso (1997). Transmembrane migration of hydrophobic channel forming peptides in lipid vesicles determined using ^{1}H and ^{2}H nuclear magnetic resonance spectroscopy. *Biophys. J. 72*, A398.
40. G. Molle, J.-Y. Dugast, H. Duclohier and G. Spach (1988). Conductance properties of des-Aib-Leu-des-Pheol-Phe-alamethicin in planar lipid bilayers. *Biochim. Biophys. Acta 938*, 310–314.
41. A. Matsubara, K. Asami, A. Akagi and N. Nishino (1996). Ion-channels of cyclic template-assembled alamethicins that emulate the pore structure predicted by barrel stave model. *Chem. Comm. 17*, 2069–2070.
42. K. Asami, A. Matsubara, A. Akagi and N. Nishino (1996). Ion-channels of alamethicins assembled with a cyclic pseudopeptide. *Prog. Biophys. Mol. Biol. 65*, suppl. l, 107, P-C3-07.

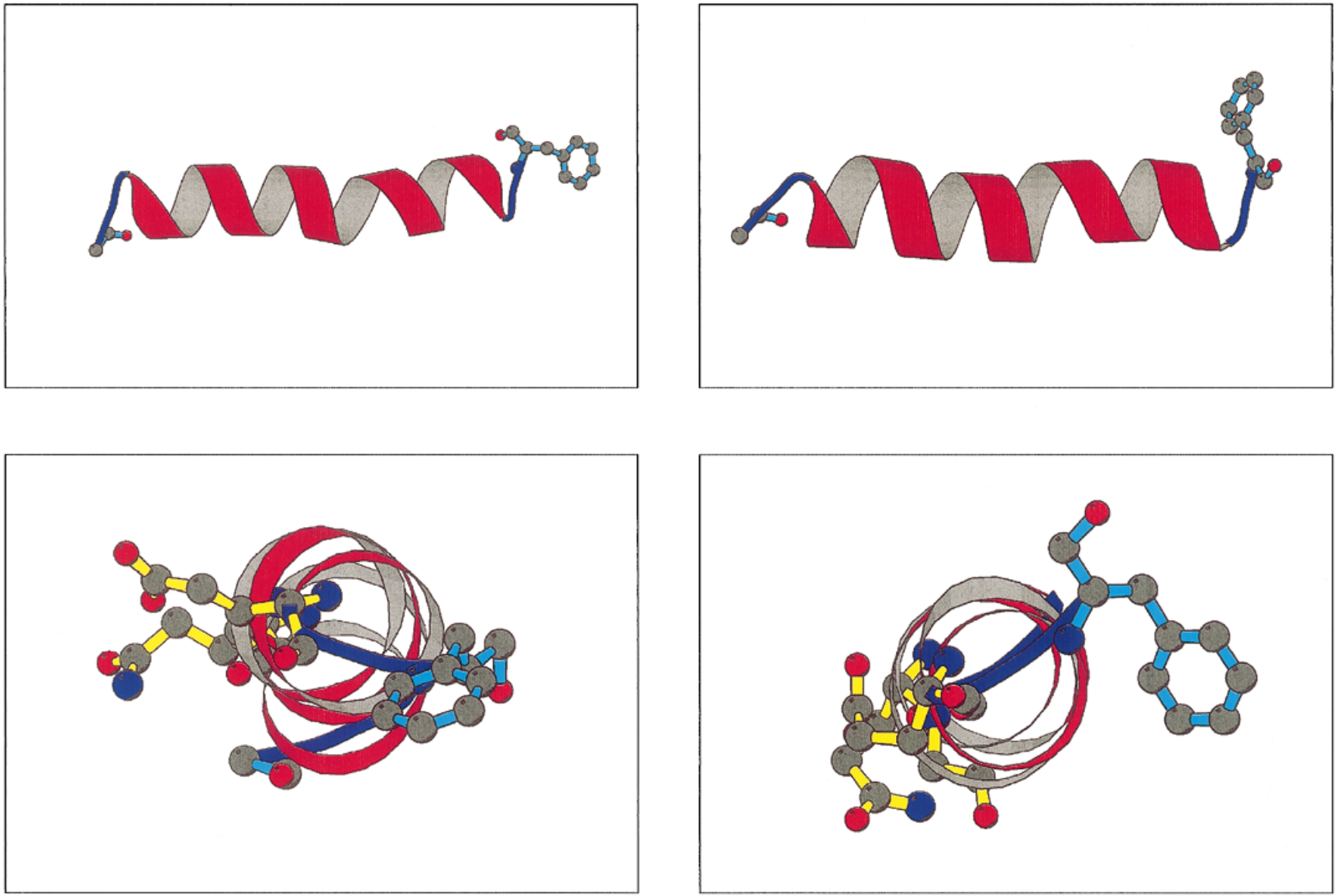

Figure 5. Average molecules of L2 computed from the 20 lowest energy structures obtained from molecular modelling (left) in methanol and (right) in SDS micelles. Only a schematic backbone ribbon is drawn (red and grey colours). Structures are shown (top) along the helical axis and (bottom) orthogonally to this axis. For all structures, lateral chains of terminal Ac0 and Pheol20 are drawn in blue colour as well as those of hydrophilic Gln7 and Glu18 residues in yellow colour for the bottom representations.

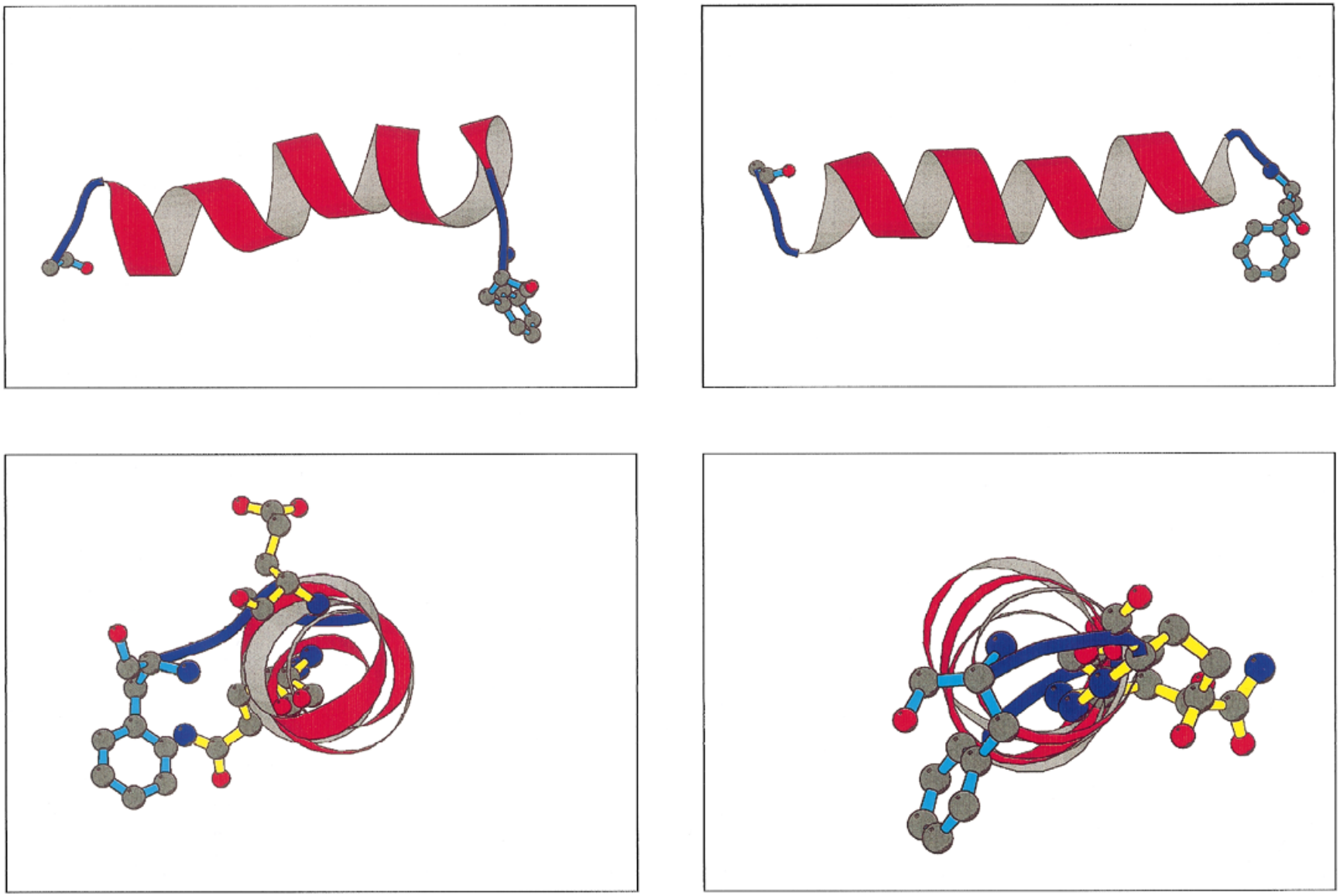

Figure 6. Average molecules of L5 computed from the 20 lowest energy structures obtained from molecular modelling (left) in methanol and (right) in SDS micelles. For most of the residues, only a schematic backbone ribbon is drawn (red and grey colours). Structures are shown (top) along the helical axis and (bottom) orthogonally to this axis. For all structures, lateral chains of terminal Ac0 and Pheol20 are drawn in blue colour as well as those of hydrophylic Gln7 and Glu18 residues in yellow colour for the bottom representations.